299 Luminal A Breast Adenocarcinoma Has Similar Rate of Metastatic Progression as Luminal B but Greater Overall and Disease Free Survival.

R Zreik, C Chisholm, C Yao, C Ruud, VO Speights. Scott & White Memorial Hospital, Temple, TX.

Background: Breast cancer has been classified into subtypes based on type of differentiation (ductal, lobular, etc) and/or immunohistochemical and fluorescence in-situ hybridization characteristics (Luminal A, Luminal B, etc). We studied patients who were found to have metastases at the time of their initial breast cancer diagnosis to evaluate overall/disease free survival and sites of metastases based on their biochemical phenotype.

Design: 108 patients with metastatic breast carcinoma at presentation were identified from 1999-2007. These were sub-typed into Luminal A (ER+/Her2-, Ki-67 <14%), Luminal B (ER+/Her2-, Ki-67 >14%), ER+/Her2+, ER-/Her2+, and triple negative (ER-/PR-/Her2-). Data was compiled regarding the histological criteria of the primary tumor, the sites of metastasis, and overall/disease free survival.

Results:

Breast Cancer Results

Variable	Luminal A (N=18)	Luminal B (N=34)	ER+/Her2+ (N=21)	ER-/Her2+ (N=10)	Triple Negative (N=25)
Histologic Type					
Ductal	13	26	18	9	24
Lobular	5	6	3	1	0
Other	0	2	0	0	1
Histologic Grade					
1	4	1	0	0	0
2	8	23	9	1	3
3	6	10	12	9	22
Survival					
Alive	4	8	6	2	2
Dead	14	26	15	8	23
Overall (months)	67	50	44	52	32
Disease Free (months)	55	37	36	35	37
Initial Site of Metastasis					
Visceral	6	22	12	7	14
Bone	15	17	13	4	12
Brain	0	0	3	1	3
Other	3	5	5	2	6
Site of Metastasis Progression					
Visceral	9	20	7	5	9
Bone	12	12	6	2	4
Brain	0	1	1	0	4
Other	3	4	41	2	8

Luminal A tumors was the second most infrequent sources of metastases. Luminal A had the longest overall and disease free survival. Luminal A most frequently metastasized to the bone at presentation (83%). ER-/Her+ tumors were the most frequent source of initial visceral metastasis (70%). Brain metastases were most commonly found at diagnosis of ER+/Her2+ (14%) and triple negative tumors (12%). Triple negative tumors most frequently spread to brain (16%).

Conclusions: Luminal A tumors, commonly thought to have a less aggressive clinical course, had more frequent bone metastases than their more aggressive counterparts. Metastatic progression involving the brain was most common among patients with triple negative tumors. Overall/disease free survival and histologic grade were the only major differences between Luminal A and Luminal B, with Luminal A having much improved survival and lower histologic grade. Rates of metastatic progression between Luminal A and Luminal B tumors were similar.

Cardiovascular

300 Progenitor Cells for Abdominal Aortic Aneurysm.

I Aboshady, D Vela, KG Khalil, LM Buja. The Texas Heart Institute, Houston; The University of Texas HSC, Houston.

Background: Current forms of treatment of abdominal aortic aneurysm (AAA) utilize open surgical repair or endovascular exclusion with a stent graft; both of which have major side effects with potentially life-threatening consequences. The aim of this study is to assess the potential role of progenitor cells in attenuating the progression, preventing rupture and providing treatment of aortic aneurysmal dilatation.

Design: AAA was induced in the infrarenal abdominal aorta of forty two 20-week old C57BL/6 Apo E -/- mice; maintained on a western diet beginning at week 4; by periarterial application of calcium chloride (0.5M). Angiotensin II was administered to dedicated groups of animals (500-1000ng/min) for 28 days via subcutaneous osmotic minipumps to enhance aneurysm growth. Stem cell antigen-1 positive, c-kit positive, Lin-negative progenitor cells; separated using immunomagnetic beads, were isolated from primary cultures of bone marrow of green-fluorescent-protein (GFP) C57BL/6 mice to facilitate tracking. Sorting of cells was done through fluorescent antibody cell sorting flow cytometry using FITC-conjugated rat anti-mouse Sca-1 antibody. Cells were injected intramurally at the site of maximum dilatation using sharpened capillary tubes to accommodate the diameter of the vessel wall.

Results: Measurements of the maximum cross-sectional diameter of the aneurysmal and normal segments of the aorta were done before and after each step; *in situ* (using a specialized calibrated digital camera), *in vivo* using state-of-the-art high-resolution micro-ultrasound imaging system (Vevo 770) designed especially for small animal imaging research and from histology (Visualsonics Inc., Toronto, Canada). Echocardiographic and digital measurements showed ~ 11.5% reduction of the mean maximum cross-sectional diameter after application of progenitor cells to the aneurysmal segments of the suprarenal aorta (mean=0.93 +/- 0.28 vs. 1.04+/-0.24 mm) and ~ 10.1% reduction (mean=0.69 +/- 0.12 vs. 0.77 +/- 0.09 mm) in the aneurysmal segments of the infrarenal aorta compared to non-aneurysmal segments and controls. Histopathologic examinations of the *ex vivo* aortic sections showed non-significant differences in measurements among the aneurysmal and non-aneurysmal segments from test groups and controls.

Conclusions: This is a less invasive, fast and potentially effective stem cell therapy to help in delaying eventual rupture of AAA. Further studies are needed to further assess and maximize the capabilities and limitations of this novel technique.

301 Integrated Microscopy Techniques for Analyzing Postmortem Intravascular Stents.

FJ Clubb, SD Darrouzet, AW Roberts, BR Weeks, M Buja. Texas A&M University, College Station; Texas Heart Institute, Houston.

Background: The use of intravascular stents in treatment of coronary artery disease represents a major means for treating coronary artery disease. Coronary stents are implanted in thousands of patients every year in the United States (650,000 in 2006). While there are many reasons for a physician to implant a stent, they, like all implanted medical devices, carry a potential for failure. Current technologies for direct evaluation of vessels with stents include radiography and light microscopy (paraffin or plastic embedding). Though these techniques are fraught with limitations. We have developed a method of integrating micro-computed tomography (microCT) with microground tissue sectioning. By integrating these two techniques, we developed an efficient and a cost effective means of examining postmortem intravascular stent implants.

Design: Human autopsy samples were collected from patients with stents implanted in the coronary arteries (n = 6). The samples were processed for high-resolution radiographs and then microCT scans performed. The vessels were then processed for microgrinding using the data from the microCT scan acquire sections in the area of interest. These microground sections allow processing to occur without decalcification of plaques or removal of the stent struts prior to sectioning, providing a clear and complete view of the state of the tissue in the area of interest. The resulting histology was then compared to the three dimensional volume.

Results: The high resolution scans of the metallic stents allow for detection of fractures in the stent struts as well as calcified plaques within the vascular wall. Such areas of interest can then be localized, allowing the pathologist exclude the vast majority of tissue from processing for histology. In all six cases, the microCT scans demonstrated complications with the stent deployment or problems that arose post-implant, which were then verified by the corresponding histology.

Conclusions: High-resolution microCT (voxel size of ~13µm) allows efficient identification of areas of interest in coronary vessels with implanted stents in a non-destructive manner. Employing MicroCT for precision-guided microground sections eliminates the need for serial sections on coronary tissue and allows for rapid localization of complications followed by microground light microscopy histology sections for examination.

302 Cardiac Pathology in Nephrogenic Systemic Fibrosis: Correlative Histopathology and Gadolinium Analysis Using Scanning Electron Microscopy/Energy Dispersive X-Ray Spectroscopy.

RL Davis, D Xia, JL Abraham. SUNY Upstate Medical University, Syracuse, NY.

Background: Nephrogenic systemic fibrosis (NSF) is a skin and frequently systemic fibrosing disorder seen in patients with impaired renal function, related to Gadolinium (Gd) release from its chelated form in MRI contrast agents. Little is known about the cardiac pathology of NSF. We review cardiac findings in 11 NSF autopsy cases sent to our lab for review and multi-organ Gd analysis.

Design: Autopsy slides containing myocardial tissue were reviewed for consensus grading of pattern and extent of calcification, fibrosis, and other findings. Analyses of tissues *in situ* in paraffin blocks using variable pressure scanning electron microscopy and energy-dispersive x-ray spectroscopy (SEM/EDS) were done by one pathologist (RLD).

Results: Patients ages range from 41-80 (median 64) yr., with 5 women, 6 men. The only consistent histopathologic findings in the hearts in these NSF autopsies are vascular calcification and interstitial myocardial fibrosis. Some cases also show calcification in cardiomyocytes. Gd deposition was detected in hearts of 11 of 11 cases examined to date using SEM/EDS. Gd-containing deposits are confirmed in vascular calcification as well as in interstitial fibrotic areas, including in fibrocytes. In some cases, the Gd-containing deposits are visible by light microscopy (confirmed by correlative LM-SEM/EDS analysis; see Figure 1). As in all tissues in NSF cases analyzed to date, the Gd deposits in cardiac tissues are in the form of insoluble Gd-phosphate-calcium compounds.

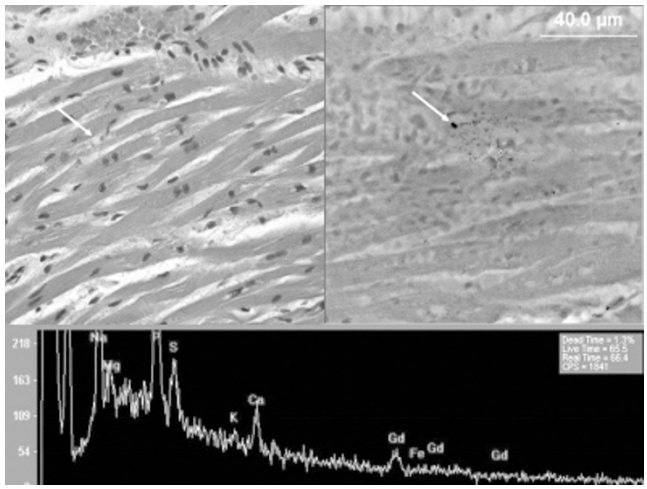

Figure 1. Myocardium, H&E showing tiny basophilic deposits in cardiomyocytes and interstitium (top left); backscattered electron SEM image of corresponding area in paraffin block with dark deposits of higher atomic number (top right); EDS spectrum collected from one of dark deposits shows peaks for Gd, Ca, P, Na (bottom).

Conclusions: Many of the myocardial changes seen in NSF may be related to tissue calcification, congestive heart failure and other changes common in advanced renal failure. Gd is known to promote formation of calcium-phosphate deposition. Whether NSF promotes more rapid and severe progression of these findings than in renal failure patients without NSF remains in need of further investigation.

303 Thrombin-Dependent NF-κB Activation and Monocyte/Endothelial Adhesion Is Mediated by a ß-Arrestin/CARMA3-Bcl10-MALT1 Signaling Complex; Implications for Atherogenesis.

PC Delekta, IJ Apel, S Gu, K Siu, Y Hattori, LM McAllister-Lucas, PC Lucas. University of Michigan Medical School, Ann Arbor; Dokkyo University School of Medicine, Mibu, Tochigi, Japan.

Background: Thrombin is a potent modulator of endothelial function, and through stimulation of NF-κB, induces endothelial expression of adhesion molecules (eg, ICAM-1 and VCAM-1). These cell-surface molecules recruit inflammatory cells to the vessel wall and thereby participate in the development of atherosclerosis, which is increasingly recognized as an inflammatory condition. The principal receptor for thrombin on endothelial cells is PAR-1, a member of the GPCR superfamily. While it is known that PAR-1 signaling to NF-κB is a key step in endothelial dysfunction, the steps leading to stimulation of NF-κB have remained unclear.

Design: Endothelial cell culture models based on the mouse SVEC4-10 and human EA.hy923 lines were used to test the role of a signaling complex composed of three principal proteins, CARMA3, Bcl10, and MALT1, in mediating NF-κB activation downstream of PAR-1. RNA interference was used to abrogate expression of each protein and the affect on NF-κB activation was assessed through detection of IκB phosphorylation, NF-κB nuclear translocation, and expression of the NF-κB gene targets, VCAM-1 and ICAM-1. In addition, the impact of Bcl10 knock-down on thrombin-responsive endothelial/monocyte adhesion was evaluated, as was recruitment of monocytes to the aortic intima of Bcl10-/- mice. Finally, the role of ß-arrestin2 was evaluated through RNA interference and through the use of MEFs derived from ß-arrestin2-/- mice.

Results: We demonstrate that a complex of proteins including CARMA3, Bcl10, and MALT1 link PAR-1 activation to stimulation of the canonical NF-κB signaling pathway. Further, we provide evidence that ß-arrestin2 serves as a scaffold to link the PAR-1 receptor to the CARMA3/Bcl10/MALT1 signaling complex. Disruption of the complex impairs thrombin-dependent induction of adhesion molecules, thereby reducing attachment of circulating monocytes.

Conclusions: The CARMA3/Bcl10/MALT1 complex shares features with an analogous CARMA1-containing complex found in lymphocytes. We now show that the CARMA3-containing complex functions in cells outside the immune system, contributing to endothelial dysfunction and recruitment of inflammatory cells. Since atherogenesis is an inflammatory condition, we are exploring the use of MALT1 inhibitors as a therapeutic approach to thrombin-dependent vascular disease.

304 CD56 (NCAM) Induces Apoptosis and Negative Inotropy in Ischemic Cardiomyopathy.

S Gattenlohner, G Ertl, C Angermann, H-K Muller-Hermelink. Institute of Pathology, Medical University of Graz, Austria; University of Würzburg, Germany; Institute of Pathology, University of Würzburg, Germany.

Background: CD56 (NCAM) belongs to the family of Ca2+-independent cell adhesion molecules, CAMs, showing abundant expression mainly in fetal neural tissues. Recently, we found that CD56 is specificially overexpressed in ischemic cardiomyopathy (ICM) and regulated by the transcription factor RUNX1 (AML1). The aim of the study was to investigate the function of the CD56 expression in ICM in particular with respect to development of heart failure.

Design: animal model for acute and chronic ischemia, RT-PCR and western Blot, stable cell transfection, micro cDNA array, FACS anaylsis and intracellular Ca+ measurements.

Results: In an animal model of acute heart ischemia we could demonstrate a complete downregulation of CD56 expression in infarcted heart tissue and its upregulation in surviving surrounding cardiomyocytes, regulated by novel RUNX1 isoforms with activating and inhibiting function on the CD56 expression. Adressing the question of its functional relevance we identified the highmolecular $CD56^{140kDa}$ isoform as the exclusively expressed CD56 isoform in failing human hearts among the known structural and functional highly different CD56 variants. In micro array cDNA chip analysis and subsequent quantitative RT-PCR using CD56 isoform specific stable transfectants of the murine cardiomyocyte cell line HL-1, the $CD56^{140kDa}$ overexpressing cardiomyoctes showed an induction of apoptosis related genes as well as downregulation of pathways related to calcium channel signalling. These data were confirmed by functional tests on human living cardiomyocytes demonstrating an increased apoptosis (5-fold) in Annexin V FACS analysis and downregulation of the proliferation in MTT assay (3-fold) as well as a reduced calcium influx (8-fold) in Fluo-4AM intracellular measurement with significantg reduction of contractility.

Conclusions: We conclude that the overxpression of $CD56^{140kD}$ is functionally relevant for the development of ICM and blocking of $CD56^{140kD}$ expression respectively its dependent signalling cascades might be a therapeutical target for the treatment of loss and insufficient contractility of cardiomyocytes in ischemic heart failure.

305 The Frequency of Pathologist Endomyocardial Biopsy Interpretation Strongly Influences Rates of Rejection.

MK Halushka. Johns Hopkins University SOM, Baltimore, MD.

Background: Many factors influence the incidence of treatable rejection after cardiac transplantation including patient age, sex, and medication adherence. Two pathologist-based variables also impact on the diagnosis of rejection. That is the differing opinions on Quilty lesions and whether a certain histologic pattern indicates diffuse, mild rejection (1B) or focal moderate rejection (3A). This project investigated a second pathologist-based variable: whether the incidence of rejection was based on the frequency by which pathologists evaluate surveillance endomyocardial biopsies.

Design: A retrospective analysis of all endomyocardial biopsy specimens taken at our institution for rejection surveillance from 2000-2009 was performed. Six pathologists, five of whom had specific cardiovascular pathology training, interpreted biopsies during this time. Three pathologists were active on the service, while the three other pathologists served in a backup capacity. The frequency of call rates for treatable cardiac rejection (3A, 3B, 2R or 3R) was determined for each pathologist.

Results: In all, 4,762 biopsies were included in this study. The frequency of treatable cardiac rejection was strongly impacted upon by the number of biopsies evaluated by a given pathologist over that time course (Table). The three pathologists who infrequently read these biopsies had a rate of 2R+ diagnoses that was nearly 3x as high as the more frequent pathologists (rejection rate 10.9% vs 3.8%, biopsies read 496 vs 4,266, $p<0.001$). Importantly, there were no large shifts in rates of rejection over the decade or significant differences in the patient population, which included adult and pediatric cases, suggesting that no extrinsic factors impacted upon these variable rates of rejection diagnoses.

Biopsy interpretation by pathologist

Pathologist	Biopsies Interpreted	Rate of 2R+	Period of activity
1	30	26.7%	2005-06
2	66	16.7%	2000-01
3	400	8.8%	2000-06
4	862	5.5%	2006-09
5	1,641	1.8%	2000-04
6	1,763	4.8%	2004-09

Conclusions: This study identifies pathologist familiarity with endomyocardial biopsy as a strong factor for the incidence of rejection diagnoses among heart transplant recipients. As with all pathology specimens, comfort with the material is based upon repetition. This data suggests that at a given institution, the interpretation of endomyocardial biopsies should be performed by a more limited number of pathologists who can establish familiarity with the material.

306 Primary Sarcoma of the Aorta and Lower Extremity Arteries: An Analysis of 26 Cases.

JE Heath, LF Xu, AP Burke. University of Maryland Medical Center, Baltimore.

Background: Primary sarcomas of the aorta and lower extremity arteries are rare. The tumors are often initially mistaken for aneurysm or atherosclerotic disease, and are therefore usually diagnosed late in the disease course. We present a series of 26 aortic and lower extremity artery sarcomas with clinicopathologic data.

Design: Data was collected retrospectively by reviewing clinical history, operative reports, histology, and immunohistochemical stains.

Results: Of the 26 cases, there were 16 men (67.7 ± 13 years) and 10 women (58.6 ± 18 years). Tumors occurred in the abdominal aorta (12), descending thoracic aorta (9), femoral artery (4), and ascending aorta (1). Presenting symptoms included claudication (8), pain (7), abdominal aortic aneurysm (AAA) (3), renal artery stenosis (1), aortic rupture (1), vasculitis (1), bowel ischemia (1), recurrence of a previously resected aortic sarcoma (1) and discovered incidentally at surgery or autopsy (3). The diagnosis was not suspected clinically in any case. The tumors were sampled by aortectomy, endoluminal excision, AAA repair, and at autopsy.

Histologically, there were 12 undifferentiated pleomorphic sarcomas (UPS), 11 epithelioid angiosarcomas, 2 angiosarcoma, and 1 osteosarcoma. Typically there was a viable layer of malignant cells facing the lumen, overlying necrotic tumor and fibrin. Immunohistochemically, epithelioid angiosarcomas were cytokeratin and CD34 positive, and UPS were positive for vimentin, and also for actin in fewer than half of the cases.

Conclusions: Aortic sarcomas have a variety of clinical presentations, and are rarely suspected clinically, with the diagnosis first made at surgical resection. Mean age at presentation is in the 7th decade, with a slight male predominance (1.6:1). There are two major histologic types, undifferentiated pleomorphic sarcoma and epithelioid angiosarcoma. The distinction between the latter and carcinoma is facilitated by immunohistochemical stains.

307 Allograft Pathology in Patients Transplanted for Idiopathic Dilated Cardiomyopathy.

T Huebner, J Heath, F Tavora, B Griffith, A Burke. University of Maryland, Baltimore; Federal University of Sao Paulo, Brazil.

Background: There are few morphologic studies of idiopathic dilated cardiomyopathy (CM) treated with transplant.

Design: We prospectively correlated gross, histologic and clinical findings of hearts explanted in a 5-year period from patients with a clinical diagnosis of non-ischemic CM, and correlated left ventricular diameter with preoperative echocardiographic reports.

Results: Of 103 consecutive allografts, the clinical diagnosis was ischemic heart disease (n=28), hypertrophic cardiomyopathy (n=4), failed allograft (n=4), amyloidosis (n=3), heart tumor (n=1), restrictive CM (n=1), and non-ischemic CM (62). In the last group, there were 41 men (51 ± 13 years) and 21 women (42 ± 18 years). The pathologic diagnosis was idiopathic (dilated) cardiomyopathy (DC) in 54 (87%), and specific cardiomyopathy in 8 (13%). Specific diagnoses were arrhythmogenic right ventricular cardiomyopathy (n=5), amyloid (n=2) and sarcoid (n=1), none of which were suspected clinically. The 54 hearts with idiopathic DC had a mean heart weight of 503 gms, (range 220-980 gms). Pathologic subsets of the DC group included 4 hearts without enlargement, cavity dilatation or significant histologic findings (minimal DC); 3 hearts with histologic evidence of healed myocarditis; and 5 hearts with features of left ventricular noncompaction. Four patients had prior mitral valve replacement to manage heart failure. There were 7 post-partum DC, 1 with a histologic pattern of healed myocarditis, and one alcoholism-associated DC. Familial DC comprised 16% (9 of 54 patients). In patients without prior assist device placement, pathologic left ventricular cavity diameter correlated with echocardiographic end-diastolic diameter (r^2 0.8, p<.0001), but there was a mean 1.7 cm underestimation pathologically.

Conclusions: Non-ischemic cardiomyopathy is heterogeneous morphologically, and unexpected diagnoses are uncovered in over 10% of cases. Left ventricular measurement at explant correlates well with echocardiographic findings, with a relatively consistent underestimation of the diameter.

308 Pathologic Analysis of Transcatheter Aortic Valve Explants.

ER Ladich, N Carter-Monroe, R Kutys, R Bonan, R Virmani. CVPath Institute Inc, Gaithersburg; Montreal Heart Institute, Canada.

Background: Transcatheter aortic valve implantation (TAVI) is a therapeutic option for high-risk patients with aortic stenosis not considered to be suitable candidates for surgical aortic valve replacement. Two primary transcatheter technologies are currently utilized: the Edwards percutaneous heart valve (PHV) (Edwards Lifesciences, Irvine, CA) and the CoreValve aortic prosthesis (Medtronic, Minnapolis, MN). Gross and histopathologic examination provide insights into the pathologic changes that occur over time in explanted valves.

Design: 11 Edwards PHV valves and 5 CoreValve explants were examined. Gross observations included prosthetic valve location, stent expansion, apposition to the aortic root and integrity of the prosthetic valve leaflets. All sections were examined by light microscopy for the presence of neointima, inflammation, calcification, thrombus/vegetations and degeneration of pericardial leaflets. In addition, clinical records were reviewed when available.

Results: Implant durations for the Edwards PHV ranged from 1 day to 4 years (age 81-91 years). The stent frames were intact and anchored in the native annulus. Histologically, there was early platelet/fibrin deposition which eventually formed a thin layer of neointima around the devices. Leaflets showed mild inflammation and over time basal pannus formation. In one acute death, there was obstruction of the left main ostium by native calcified leaflet evulsing over the device. A Type I aortic dissection associated with extensive nodular calcification of the native leaflets was identified at 3 years. One valve showed infective endocarditis. The 5 CoreValves had postimplant times ranging from 3 days to 350 days (age range: 77-85 yrs). The self-expanding frames conformed to the aortic root with patent coronary ostia. The mitral leaflet was intact in all explants. Postmortem analysis showed early platelet/fibrin deposition and formation of thin pannus over time. One autopsy case (3 days) showed a perforation in the aortic root close to the left main ostium. Another device was placed too low with a valve in valve implanted as bail out. There was thick pannus formation around leaflet bases in one patient with cardiac amyloidosis (350 days).

Conclusions: There were no device fractures even as late as 4 years. Tissue growth around the devices, leaflet inflammation, basal leaflet pannus growth, and endocarditis were similar to those previously reported for surgically implanted valves. The degree of native leaflet calcification may play a role in early and late complications and deserves further study.

309 Pathologic Identification of Foreign Materials Associated with Cardiovascular Interventional Devices.

ER Ladich, N Carter-Monroe, F Kolodgie, M Olson, R Virmani. CVPath Institute Inc, Gaithersburg.

Background: Foreign materials associated with cardiovascular interventions include metals and wires, polymers for drug delivery, hydrogel coatings, plastic sheaths, and gauze; these have a possibility of distal embolization. Herein we describe some pathologic consequences associated with dislodgement and embolization of foreign materials used routinely in cardiovascular technologies.

Design: Our laboratory processes a large numbers of cardiovascular devices in various locations such as coronary arteries, peripheral vasculature, myocardium and other organs. Multiple sections of distal myocardium and organs were taken at the time of explantation to determine the presence or absence of emboli. Scanning electron microscopy and spectroscopy were performed in cases where foreign materials were identified to determine the composition of the material.

Results: A variety of foreign materials were identified in vascular, myocardial and organ sections following cardiac interventions. 1) Basophilic non-polarizable material morphologically consistent with hydrogel has been identified in several anatomic locations. Fragments of hydrogel were seen in small intramyocardial arteries following coronary stenting. In addition, hydrogel fragments were identified within the cavernous sinus of a carotid artery with a cerebral coil implant. Another case showed hydrogel fragments and Teflon coating in the left atrium surrounding a trans-septal puncture site. 2) Plastic fragments, presumably originating from the introducer sheath, were identified in myocardial sections associated with granulomatous inflammation. 3) Dislodged fragments of stent polymer were found adjacent to struts eliciting a granulomatous reaction as well as within distal myocardium. 4) Myocardial sections showed small polarizable fragments consistent with cotton fibers surrounded by granulomatous inflammation and giant cells.

Conclusions: Coronary and peripheral arterial interventions produce morphologic changes that are influenced by the procedure or device used. In approaching such cases, the pathologist must be knowledgeable about the devices and delivery systems used and the potential for foreign materials associated with these technologies to embolize. Special studies such as scanning electron microscopy and spectroscopy may be required to elucidate the composition of these foreign materials.

310 Clinicopathological Significance of Microvasculopathy after Heart Transplantation.

L Li, H Wang, L Song, Y Guo, J Zhang, J Huang, H Zhao. Chinese Academy of Medical Sciences, Peking Union Medical College, Cardiovascular Institute, Fu Wai Hospital, Beijing, China.

Background: Stenotic microvasculopathy is common after heart transplantation; however, the associated risk factors and predictive value of stenotic microvasculopathy after heart transplantation for the development of cardiac allograft epicardial vasculopathy and reduced cardiac function are still unclear and controversial.

Design: 278 endomyocardial biopsy specimens were harvested from 64 patients one year later after heart transplantation. Light microscopic evaluations were performed for microvasculopathy, defined as stenotic endothelial and/or medial disease. Epicardial vasculopathy was evaluated by coronary angiography, and/or intravascular ultrasound. The relationship between stenotic microvasculopathy and eipcardial vasculopathy, cardiac function, recipient age, times of acute cellular rejection and grade, Quilty lesion, coronary atherosclerosis, and diabetes mellitus was also investigated.

Results: Stenotic microvasculopathy was present in 38 of 64 patients (59%) and was due to medial (30/38; 79%) rather than endothelial disease (2/38; 5%) or a combination of both (6/38; 16%, $P<0.001$). Patients with stenotic microvasculopathy were younger than that without stenotic microvasculopathy (40.68±15.85 *vs* 49.42±8.67, $P=0.013$). The numbers of acute cellular rejection (0.64±0.43 *vs* 0.37±0.32, $P<0.001$) and ≥ grade 2 acute rejection (0.84±0.16 *vs* 0.23±0.10, $P=0.007$) were greater in stenotic microvasculopathy group compared to that of non-stenotic group. Multivariate regression analysis demonstrated that the recipient age (r=-0.05, $P<0.001$) and acute rejection grade (r=3.40, $P<0.001$), rather than Quilty lesion, coronary atherosclerosis, and diabetes mellitus are significant risk factors for developing microvasculopathy after heart transplantation. Microvasculopathy observed in endomyocardial biopsies after heart transplantation was not related to epicardial vasculopathy and reduced cardiac dysfunction.

Conclusions: Microvasculopathy is a frequent immune-mediated event after heart transplantation. The occurrence of microvasculopathy is not a predictive index for developing allograft epicardial vasculopathy and worsening cardiac function. The clinicopathological significance of long term observation of microvasculopathy after heart transplantation is warranted.

311 Pathological Evaluation of Endomyocardial Biopsies from Transplanted Hearts – Utilization of Automated Whole Slide Imaging for Quality Assurance.

LAM Matzke, AJ Ostry, BM McManus, MF Allard. University of British Columbia, Vancouver, Canada; St Paul's Hospital, Vancouver, BC, Canada.

Background: Modern automated whole slide imaging (WSI) systems have great potential as clinical, educational and research tools in pathology. One potential benefit is the use of such systems in telepathology. Prior to widespread usage of WSI systems for telepathology, the impact of this technology must be evaluated with respect to quality assurance (QA) of diagnoses rendered from samples evaluated. In this project, we examined the use of automated WSI systems for surgical pathology with regard to QA for the pathological evaluation of endomyocardial biopsies (EMB) from heart allografts.

Design: Sixty EMB from transplanted hearts that were previously examined by a pathologist using traditional light microscopy (LM) were selected randomly from all EMB accessioned between 2009 and early 2010. A diagnosis based on the 2006 ISHLT scoring system was previously rendered on each case by one of three pathologists (AO, BM, MA) with training and expertise in cardiovascular and transplantation pathology. The sixty cases (20 for each pathologist) were blinded and automated WSI capture was performed on an Aperio ScanScope XT Scanner (Aperio Technologies, Vista, CA)

located at St. Paul's Hospital. WSI for each case were produced and each pathologist re-evaluated their 20 cases and rendered a new diagnosis. These results were compared to an earlier intra-observer evaluation study comparing score concordance based solely on LM (2 pathologists; evaluating 4 and 5 cases respectively).
Results: Concordance rates based on LM versus WSI methods ranged from 14/20, 18/20 to 20/20 cases. Weighted Kappa score evaluation was applied to calculate intra-observer variation between the two diagnostic methods, the results of which correspond to moderate to very good agreement. Concordance rates based solely on LM ranged from 3/4 to 4/5 cases, both corresponding to good agreement. Following the case analyses, all pathologists were asked to critically comment on the benefits, drawbacks and challenges in using the two methodologies.
Conclusions: This study evaluated quantitative and qualitative QA aspects using WSI technology for pathological evaluation of EMB suggesting that, with further consideration, the WSI approach has the potential in enabling telepathology as an important tool in the remote pathological evaluation of cardiac specimens as well as for QA and consultation purposes. Such utility will ultimately lead to more effective, quickly available patient care.

312 Gene and Protein Expression in the Myocardium Varies with Duration of Mechanical Circulatory Assistin Heart Failure Patients.

A Meredith, A Samra, L Matzke, C Leung, B McManus. University of British Columbia, Vancouver, Canada.
Background: Management of the failing heart involves medical therapy, mechanical circulatory assist(MCA) devices and heart transplantation. Unloading of the heart by MCA may induce reverse remodeling andnormalize cardiac parameters (cardiac chamber geometry, size, volume, ejection fraction and fetal gene expression).We undertook to identify gene and protein markers of heart failure and determine "fetal" gene and proteinexpression within the heart upon MCA. We examined the hypothesis that expression changes over timecorresponding to the duration of circulatory support with MCA.
Design: Left ventricular (LV) apical tissue cores removed during LV assist device (LVAD) implantation, andcorresponding explanted hearts obtained at the time of transplantation were examined. Tissues from seven patientswith a mean age of 55.6 ± 5.4 years were analyzed. Serial sections were prepared with standard histology stainsfor quantification of myocardial fibrosis and remodeling. Immunohistochemical staining for markers of myocardialdysfunction and remodeling (brain natriuretic peptide, galectin-3, versican, matrix metalloproteinases 2 and 9) wasperformed. Extracted RNA was analyzed on Affymetrix GeneChip Human Genome U133 Plus 2.0 Arrays and byquantitative PCR for α-myosin heavy chain, β-myosin heavy chain and phospholamban. Differential staining, geneexpression and degree of remodeling were quantified and correlated with duration of MCA. Comparison was alsomade of gene and protein signatures from LV core samples at time of LVAD implant with apical LV samples fromcorresponding explanted hearts.
Results: Deleterious LV remodeling and alterations in contractile function in HF are associated withchanges in gene and protein expression, including activation of the "fetal" gene program, and dysregulatedexpression of fibrotic markers. Unloading of the heart through MCA results in decreases in myocyte hypertrophyand myocardial fibrosis with concomitant changes in gene and protein expression.
Conclusions: In conclusion, the extent of geneand protein expression alteration is a function of duration of mechanical unloading, and a time dependent alterationin relevant markers exists.

313 Antibody-Mediated Rejection in Heart Transplantation: Characterization of Patients with C4d Immunoreactivity in Endomyocardial Biopsies.

MK Mirza, SE Fedson, Y Chi, AN Husain. The University of Chicago, IL.
Background: C4d is widely accepted as a marker for antibody-mediated rejection in cardiac allografts; however its usefulness as a prognostic marker is under debate. The aim of this prospective study was to determine the significance of C4d immunoreactivity in endomyocardial biopsies by correlating with cardiac dysfunction, cardiac allograft vasculopathy (CAV) and death.
Design: 1771 biopsies from 200 heart transplant patients were stained prospectively by IHC for C4d deposition on paraffin-embedded tissue using anti-human C4d polyclonal antibody. Strong diffuse endothelial staining was considered positive. Cardiac dysfunction at the time of positive biopsy was evaluated by echocardiography and intracardiac filling pressures. Patients were followed for 1-6 years.
Results: Positive staining of C4d was present in 43 biopsies (2.4%) from 25 patients (12.5%). The average time from transplant to the first episode of C4d positivity was 365 days (ranging from 8 to 986 days). 9 patients had clinically significant cardiac dysfunction at the time of positive biopsy (13 out of 43 positive biopsies). 14 patients (7%) died, 7 of whom (50%) had cardiac dysfunction at the time of positive biopsy. Autopsy was performed on 6 patients; in this subset, mean time duration between transplant and death was 1213 days (ranging from 66 to 2110 days) and between first episode of C4d positivity and death was 640 days (ranging from 2 to 1193 days). CAV was noted in all 6 patients (100%).
Conclusions: C4d positivity correlated with poorer outcomes. 14 out of 25 patients who showed C4d positivity died (56%) (Institutional 5-year post-transplant survival is 78%). The outcome is even worse when C4d positivity is associated with cardiac dysfunction (100% mortality).

314 Histo-Molecular Analysis of 25 Cases of Arrhythmogenic Right Ventricular Cardiomyopathy.

V Nair, J Butany. Hamilton Health Sciences, Hamilton, Canada; McMaster University, Hamilton, Canada; University Health Network, Toronto, Canada; University of Toronto, ON, Canada.
Background: Analyze histopathological changes in the hearts with a diagnosis of ARVC; study the incidence of PKP2 mutation in this population and to characterize if possible the histological changes associated with the mutation.
Design: All ARVC cases diagnosed in the past 20 years were reviewed. Clinical data including the patient's age, sex, were recorded. PKP2 mutation analysis was done on all the cases.
Results: There were 3 autopsy cases, where the patients had a sudden death due to ARVC while 22 were surgical explants. The age ranged from 18 to 66 years. There were 16 females and 9 males. The hearts weighed from 260 to 816 grams. Right ventricular thinning was seen in 24 cases, while 14 cases showed an apical aneurysm. Fibro fatty infiltration of the right ventricle was seen in 24 cases, predominantly fat infiltration was seen in six cases while one case showed only fat infiltration. Fibrosis of the trabeculae carne was seen in 22 cases. Lymphocytes in the right ventricle were seen in 5 cases. Fibrosis of the left ventricle was seen in all 25 cases. (Subepicardial band like fibrosis was in 5cases, subendocardial fibrosis in 4, mid ventricular in 1.transmural in one and the rest showed an interstitial pattern.) Myocyte disarray was seen in 6 cases. Myocarditis was seen in 12 cases (2 cases of active myocarditis, 2 cases of eosinophilic, 1 borderline, 1 healing). Significant fibrosis involving the atria was seen in 18 cases. PKP 2 mutation was seen in 23 of 25 cases (92%). All mutations have previously been described. 14 cases (56%) had a mutation in the intronic site with no change in protein. 9 (36%) cases showed mutation on an exon that might have changes of protein.(4 of these cases had an additional mutation in the intronic site).

Table 1.

	Mutation in intron	Mutation in exon
Female to male ratio	5:2	5:4
Age	18-65yrs(Average41.5)	35-50yrs(Average42.5)
Heart weights	260-590gms(Average425)	295-815gms(Average555.5)
Myocarditis	5 cases	6 cases

Conclusions: PKP2 mutation was seen in 92% of our ARVC cases. Mutations in an exon that might have changes in the proteins were seen in 36% of cases. The female to male ratio was lower in cases with mutation on exon. No significant difference was seen in the average age, involvement of the ventricles or the incidence of myocarditis in cases of either category.

315 Immunohistochemical Expression of Prosaposin in the Normal Arteries and Atherosclerosis.

SJ Park, CH Lee, JR Kim, JH Choi. Yeungnam University College of Medicine, Daegu, Korea; Yeungnam University College of Medicine, Aging-Associated Vascular Disease Research Center, Daegu, Korea.
Background: Prosaposin, a glycoprotein encoded by a single locus on human chromosome 10, is the precursor of four sphingolipid activator proteins named saposin A, B, C, and D that activate the hydrolysis of sphingolipids by lysosomal hydrolases. It is an intriguing, ubiquitous, and highly conserved protein believed to be involved in a variety of biological processes. To investigate the role of prosaposin on the vascular aging and atherosclerosis, we analyzed expression of prosaposin in normal young arteries, normal old arteries, and atherosclerosis.
Design: Eighteen cases of normal young arteries (aged 1 to 38 years), eighteen cases of normal old arteries (aged 47 to 70 years), and eighteen cases of atherosclerosis were selected from surgically resected specimens at Yeungnam University Hospital during from 2002 to 2009. Immunohistochemical stain for prosaposin was done. Expression of prosaposin was scored semiquantatively by the intensity and proportion of immunostaining.
Results: All normal young arteries showed no expression of prosaposin (0 of 18 cases, 0%). Normal old arteries showed increased expression of prosaposin (6 of 18 cases, 33%). Prosaposin was expressed in the cytoplasm of smooth muscle cells and endothelial cells and the vascular wall in normal old arteries. All atherosclerosis cases showed markedly increased expression of prosaposin (18 of 18 cases, 100%). Expression of prosaposin was present in the cytoplasm of smooth muscle cells and macrophages, and the atheromatous plaque in the atherosclerosis.
Conclusions: Our findings suggest that prosaposin might be play a role in the progression of vascular aging and the development of atherosclerosis.

316 The Predictive Utility of Lipofuscin and Fibrosis on Endomyocardial Biopsy in Adolescents and Young Adults.

SJ Parson, SD Russell, MK Bennett, JM Dunn, N Aggarwal, S Rao, C Harrington, T Beck, MK Halushka. Saba University SOM, The Bottom, Saba, Netherlands Antilles; Johns Hopkins University SOM, Baltimore, MD.
Background: The amount of interstitial fibrosis and lipofuscin present in endomyocardial biopsy samples are thought to indicate the chronicity of heart failure. Fibrosis is known to increase in the failing heart. Lipofuscin is known to increase with age, but its relationship to heart function is unknown. This study was undertaken to determine if lipofuscin or fibrosis had predictive utility in indicating recovery of function or adverse event (death, transplant, assist device placement) at one year post-biopsy in adolescents and young adults.
Design: A retrospective analysis was performed for all non-transplant endomyocardial biopsies performed at our institution from 2000-2009 on individuals aged 10-40. Clinical and demographic information including ejection fraction (EF), EF at one year, cardiac index, death, transplantation, assist device use, sex and ethnicity were obtained as available. The degree of fibrosis was taken from the surgical pathology

record. The amount of lipofuscin was scored retrospectively in a blinded fashion on all biopsies. Linear regression and Cox proportional hazard models were used for multivariable analysis.
Results: In all, 201 biopsies were included in the study. As expected, increasing lipofuscin strongly correlated with patient age ($p<0.0001$). Surprisingly, higher levels of lipofuscin were correlated with higher EF scores at one year ($p=0.02$). This remained significant ($p=0.01$) after adjusting for age. More fibrosis was associated with lower EF at one year ($p=0.04$), although it became nonsignificant after age adjustment. Increased fibrosis, but not lipofuscin, predicted having an adverse event by one year ($p=0.02$).
Conclusions: The endomyocardial biopsy can be used to diagnose disease at the time of biopsy. This is the first study to incorporate lipofuscin as a histologic finding to predict heart function at one year. Our study demonstrates that in an adolescent and young adult population, both lipofuscin and fibrosis can prognosticate how well a patient's heart will be functioning in one year. This information can be used to help clinicians devise treatment plans for individuals in this age group.

317 Cardiac Magnetic Resonance Features of Biopsy Proven Endomyocardial Diseases and Hypereosinophilic Syndrome.

M Perazzolo Marra, S Rizzo, M De Lazzari, F Corbetti, S Iliceto, G Thiene, C Basso. Padua, Italy; University of Padua Medical School, Italy.
Background: Hypereosinophilic syndrome (HES) is characterized by marked eosinophilia and eosinophil-mediated organ damage, in the absence of primary causes. Endomyocardial pathology of HES includes eosinophilic myocarditis (EM)-Loeffler endocarditis (LE) and endomyocardial fibrosis (EMF), which are considered different stages of the same disease. Cardiac magnetic resonance (CMR) data on LE/EMF are still missing.
Design: Patients with a clinico-pathologic diagnosis of HES and/or endomyocardial diseases who underwent to CMR with late gadolinium enhancement (LGE) and endomyocardial biopsy (EMB) during the same hospitalization in the time interval 2002-2010 were enrolled. Cases with allergic, infective, autoimmune and vasculitis conditions were excluded. A complete CMR protocol (including T1 and T2 weighted images, post-contrast sequences for LGE evaluation) was performed. EMB was performed from the right ventricle (RV) and processed for histology, immunoistochemistry and polymerase chain reaction.
Results: Eight patients were studied (5 males; 42±11 y, range 25-19), including 5 with EM/LE and 3 with EMF. Molecular pathology investigation ruled out viral genomes, except for 1 case who was positive for PVB19. *Among the 5 EM/LE patients*, all but one with HES, CMR showed a moderate left ventricular (LV) dysfunction/dilatation in all; RV dysfunction/dilatation in 50%; and LV hypertrophy, myocardial edema and pericardial effusion in all. A LGE was found in LV in all, but never in RV. Endocardial thrombosis was detected in all (4 RV, 1 LV). *Among the 3 EMF patients*, 1 of whom with documented previous HES, CMR showed RV dilatation/dysfunction with free wall thickening and subendocardial LGE in all, associated with LV LGE in one. One case of chamber obliteration was found. In three EM/LE pts, CMR was repeated during the follow-up showing biventricular dilatation/dysfunction, RV LGE, normalization of LV wall thickness and subendocardial LV LGE in keeping with EMF, as confirmed by a second EMB in two cases.
Conclusions: In endomyocardial diseases with/without HES, CMR is an important diagnostic tool which allows identification of myocardial inflammation, mural thrombi and endocardial fibrosis, besides morpho-functional cardiac evaluation and confirms that EMF and EM/LE are different stages of the same disease process. The non-invasiveness supports its role in the follow-up evaluation.

318 Pathology of the Specialized Conduction System in Familial Lenègre Disease Due to SCN5A Mutations.

K Pilichou, E Carturan, C Basso, G Thiene. University of Padua, Italy.
Background: Progressive cardiac conduction (Lenègre) disease is one of the most common cardiac conduction disturbances due to degenerative changes of the specialized conducting tissue. It constitutes the substrate for bundle branch block and QRS complex widening leading to complete atrioventricular (AV) block at risk of syncope and sudden death. Recent studies indicate that SCN5A loss-of-function mutations account for a familial form of Lenègre disease.
Design: Detailed conduction system investigation by serial section technique was performed in 2 unrelated index cases (M, 35; M, 40) with previous history of syncope and an *in vivo* diagnosis of AV conduction disturbances, who died suddenly. SCN5A genetic screening was undertaken in 23 family members (13M and 10F). Full clinical evaluation through non- invasive and invasive diagnostic tools was carried out on both probands and their family members respectively.
Results: Severe fibrosis of the bifurcating His and proximal bundle branches with sclerotic interruption of the right bundle branch was determined in probands cardiac tissue at post mortem examination. Genetic screening of family members identified a nonsense mutation in exon 11, E473X (12 carriers, family A) and a missense one on exon 21, E1225K (3 carriers, family B). ECG of 15 SCN5A mutation carriers (2 probands were obligated carriers, 9 M and 6 F, age 38,4±17 yrs, range18-72) was analyzed. None of the non carriers had PQ interval prolongation. Twelve mutation carriers (80%) presented a right ventricular conduction delay and one (6,6%) a first degree left bundle branch block. Mean PQ interval was 211±36 msec. A PQ interval > 200 msec was present in 10 (67%) (mean 232±20 msec, mean age 46,5±15 yrs vs 22,2±4,9 yrs with normal PQ interval, $p=0.0004$). A QRS complex >110 msec was present in 11 subjects (mean 132±16 msec, mean age 43±17 yrs vs 26±6 yrs with normal QRS duration, $p=0.01$). A coved ST-segment elevation >2 mm in V1-V2 was present in six cases (40%). Two SCN5A mutation carriers presented normal ECG.
Conclusions: An organic substrate underlies SCN5A-associated Lenègre disease, consisting of sclerotic interruption of the bifurcating His and the proximal bundle branches in young people. Family members investigation highlighted the presence of a heritable "age-related" alteration in the conduction system.

319 Analysis of PRKAR1A Gene Locus in Sporadic Cardiac Myxomas.

S Radio, Y Zhang, D Huang, R Neff, J Bridge. University of Nebraska Medical Center, Omaha.
Background: Cardiac myxoma most frequently arises sporadically, but it may also occur as a feature of the autosomal dominant disorder Carney complex syndrome (CCS). Mutations of the tumor suppressor gene PRKAR1A represent an underlying cause of CCS which includes myxomas in multiple sites, spotty pigmentation and endocrine overactivity. Cytogenetic studies of cardiac myxoma are rare, but to date 17q23-24, the chromosomal locus of PRKAR1A, has not been shown to be karyotypically rearranged. To the best of our knowledge, molecular cytogenetic studies for the examination of submicroscopic or cryptic anomalies have not yet been conducted.
Design: Five cases of histologically confirmed cardiac myxoma with paraffin blocks available were identified from the files of the Cardiovascular Registry at UNMC. Conventional cytogenetic analysis was performed on one of these from a 71 year old male. Selection and labeling of a 192 kb bacterial artificial chromosome (BAC RP11-120M18) clone designed to span the PRKAR1A (17q23-24) locus was carried out for higher resolution analysis. After establishing the specificity of the probe and coupling it with a copy number control probe (CEP 17), dual color FISH studies were performed to assess the PRKAR1A copy number on representative paraffin-embedded tissue sections from the cytogenetically analyzed cardiac myxoma as well as 4 other cardiac myxomas (2Males, 2 Females, mean age 68) and one negative control.
Results: A hypodiploid clone with loss of chromosomes 21 and 22 accompanied by the presence of telomeric associations involving chromosome 16 and various partner chromosomes was identified in 16 cells of the karyotypically analyzed myxoma. FISH studies revealed homozygous loss of the PRKAR1A locus in one myxoma from a 74 year old female. The other 4 were negative for loss by FISH.
Conclusions: Deletion or loss of the PRKAR1A locus is demonstrated in a case of sporadic cardiac myxoma, supporting a tumor suppressor role for this gene in non-CCS associated cardiac myxomas.

320 Decellularized Porcine Aortic Roots: Histopathology Features in an Experimental Animal Model of Right Ventricular Outflow Tract Reconstruction.

S Rizzo, L Iop, A Gandaglia, M Marchini, M Spina, G Thiene, G Gerosa, C Basso. University of Padua, Italy; University of Udine, Italy.
Background: The ideal valve conduit for right ventricular outflow tract (RVOT) reconstruction is still missing. Structural valve deterioration due either to immunological reactions or dystrophic calcification is still a major challenge.
Design: TRICOL de-cellularized porcine α-Gal negative aortic roots were used to replace RVOT in nine 12 month old vietnamese pigs. As a control group, four animals had their RVOT resected and immediately reimplanted (sham operation). Both groups underwent serial echo evaluation prior to surgery, at 15 days, and every 3 months. The explanted valved conduits were analysed by histology, immunohistochemistry and electron microscopy.
Results: Intraoperative deaths occurred in 2 cases and 1 controls, excluded from further analysis. In the study group, death due to graft-related causes occurred in 2 (i.e. infective endocarditis 48 days and 9 months after implantation), whereas the remaining 5 survived with a favourable outcome and proper growth of implants (up to 35% increase in diameters) and limited inflammation. Only in 1 case (6 month after implantation) vimentin+ and α-SMA+ interstitial cells were observed within the leaflets, showing ultrastructurally collagen fibrillogenesis and elastogenesis; in the remaining cases (at 6 and 12 months) very few vimentin+ and α-SMA+ cells were detected within the leaflets, mainly at insertion level. Endothelization (CD31+ and vWF+) was evident only at insertion level, whereas the free margins of the leaflets were not covered by endothelial cells. Thrombus deposition and features of subacute infective endocarditis were detected on the luminal surfaces in 3 cases. Tissue positivity for stem cell markers and cell pattern of graft derived-primary cultures suggested cell repopulation originating from recipient bone marrow mesenchymal stem cells.
Conclusions: α-Gal negative TRICOL decellularized porcine aortic roots might represent a valuable solution for RVOT reconstruction. Although these glutaraldehyde-free valved vascular conduits seem permissive for spontaneous cell repopulation and tissue growth, the incomplete re-endothelialization with the high incidence of thrombus formation and infective endocarditis suggests the need of further studies to assess the late re-cellularization and growing capabilities.

321 Relation of Aortic Valve Weight to Severity of Aortic Stenosis: A Clinico-Pathologic Study on Surgical Specimens.

S Rizzo, R Razzolini, S Longhi, G Tarantini, M Napodano, E Abate, C Fraccaro, S Iliceto, G Gerosa, G Thiene, C Basso. University of Padua Medical School, Italy.
Background: The purpose of this study was to analyze the relation of aortic valve weight to both transvalvular gradient and area, with special regard to valve anatomy, size of calcific deposits, gender and body size.
Design: A total of 242 surgically excised stenotic aortic valves of patients (139 male, mean age 72±9 years) who had undergone preoperative cardiac catheterization and echocardiograms were weighed and examined with respect to the number of cusps (tricuspid vs. bicuspid), size of calcium deposits ("microaggregates" ≤4 mm vs. nodular "macroaggregates" >4 mm) and presence of cholesterol clefts. The relation between valve weight, gradient and area was studied.

Results: The transvalvular gradient was independent of gender or valve anatomy, and was linearly correlated with valve weight, either absolute ($r = 0.33$; $p < 0.01$) or normalized by body surface area ($r = 0.40$; $p < 0.01$). No correlation was evident between valve area and weight. Calcium macroaggregates were mainly present in males (51%) and in bicuspid valves (67%), and they were seen to be strong determinants of valve weight (2.84±1.03 g with macroaggregates vs. 1.63±0.56 g with microaggregates, $p < 0.001$), but not of transvalvular gradient. Calcium microaggregates characterized tricuspid valves (62%), where transvalvular gradient was determined by valve weight ($p = 0.0026$). Finally, the heavier the valve the less frequent were hypercholesterolemia, valve cholesterol clefts, hypertension and diabetes mellitus.

Conclusions: In aortic stenosis due to dystrophic calcification, valve weight significantly correlates with transvalvular gradient when calcific deposits are arranged in diffuse microaggregates, a condition more commonly found in tricuspid valves and in females. Nodular calcium macroaggregates add to weight but not substantially to the severity of stenosis. Surprisingly, both valve weight and valve area were independent of plasma cholesterol concentration and cholesterol cleft deposits on the leaflets, suggesting that, once aortic stenosis is established, removing risk factors may have no influence on the severity of the disease.

322 Inflammatory Activity in Sympathetic (Stellate) Ganglia of Patients with Life Threatening Cardiac Arrhythmias.

S Rizzo, D Troost, C Basso, G Thiene, A Driessen, AA Wilde, AC van der Wal. University of Padua, Italy; Academic Medical Center, University of Amsterdam, Netherlands.

Background: Long QT syndrome (LQTS) and catecholaminergic polymorphic ventricular tachycardia (CPVT) are electrical diseases of the heart characterized by episodes of life threatening arrhythmias. The pathogenesis of these inherited diseases is complex; a link to autonomic imbalance has been established, possibly as an epiphenomenon that could relate to exaggerated symptomatology. Stellate ganglion excision is a therapeutic modality in those LQTS/CPVT patients with arrhythmias that are resistant to pharmacological drugs. We investigated potential inflammatory/degenerative pathology in stellate ganglia of LQTS/CPVT patients with intractable arrhythmias.

Design: Surgically excised stellate ganglia were retrieved from 10 patients (7F, 3M, mean age 20.7±15.5 yrs) with either LQTS (n=5) or CVPT (n=5). Control stellate ganglia were obtained from 4 accidently (traumatic) deceased patients (1F, 3M, mean age 20.5±3.8 yrs). Sections were immunostained with antibodies anti S100, CD3 (pan T-cell), CD8 (cytotoxic T-cells, CTL's) Granzyme B (activated CTL's), CD20 (B-cells), and CD68 (macrophages) and MHC class II antigens. The inflammatory process was semiquantitatively graded as 0 (normal), 1 (individual inflammatory cells), 2 (inflammatory cells without ganglionits) and 3 (clustering of inflammatory cells and ganglionitis).

Results: Stellate ganglia of LQTS/CVPT patients revealed microscopic foci of score 2-3 inflammation in all cases. The infiltrates were composed of macrophages (CD68+) and T cells (CD3+) which were predominantly CD8+, Granzyme+ CTL's. B-cells were sparse. In addition, all cases showed T-lymphocytes surrounding the cytoplasm of one or more ganglion cells in combination with HLA-DR positivity, interpreted as low grade inflammatory-mediated destruction of ganglion cells (ganglionitis). Control ganglia of accidental deaths showed at maximum a mild inflammatory infiltrate (score 0-1) with sparse $CD8^+$ T cells.

Conclusions: Our findings indicate a low grade CTL-mediated ganglionitis in the stellate ganglia of severely symptomatic LQTS/CVPT patients. Production of inflammatory cytokines and a sympathetic stress response could favour cardiac electrical instability in these patients genetically predisposed to arrhythmias.

323 Strong Tranthyretin (Prealbumin) Immunostaining in Cardiac Amyloid Deposits, a Potential Pitfall for Surgical Pathologists.

AA Satoskar, Y Efebera, A Hasan, S Brodsky, A Dogan, T Nadasdy. The Ohio State University, Columbus; Mayo Clinic, Rochester, MN.

Background: Although systemic amyloidosis often presents first with renal disease, cardiac involvement usually determines the patient's prognosis. Heart involvement is common in AL type and transthyretin (ATTR) amyloidosis, and distinguishing between these two types is critical because prognosis and treatment differ greatly. Our study demonstrates the unreliability of transthyretin immunostaining in cardiac amyloid typing, even if it is strongly positive.

Design: From January 2003 to August 2010, we retrieved 229 native endomyocardial biopsies, out of which 24 were diagnosed as cardiac amyloidosis. Immunohistochemistry for kappa and lambda light chains, transthyretin (prealbumin) and serum amyloid A protein were performed on formalin fixed paraffin-embedded tissue sections. The staining of the amyloid deposits was graded as weak (trace to 1+); or strong (2 to 3+). Mass spectrometry (MS) based proteomic typing of microdissected amyloid plaques was performed on selected cases.

Results: Fifty-three percent (8/15) patients with monoclonal gammopathy/plasma cell dyscrasia showed strong transthyretin staining in the cardiac amyloid deposits (Table 1).

Table 1. Strong TTR and light chain staining in cardiac amyloid deposits.

	Strong TTR staining present	Strong light chain staining present	Both TTR and light chain staining strong
MG/PD present (n=15)	8	6	4
MG/PD absent (n=8)	6	3	3
No followup (n=1)	1	0	0

TTR=transthyretin; MG=monoclonal gammopathy; PD=plasma cell dyscracia

MS was performed in five out of these 8 cases with strong transthyretin staining, and all five revealed AL type amyloid. Three of the confirmed cases, did have concomitant strong staining for kappa or lambda light chain, but two did not stain for light chains. Among the 15 cases with plasma cell dyscrasia, only six biopsies showed strong staining for the corresponding monoclonal light chain.

Conclusions: Strong false positive staining for transthyretin is a potential pitfall in subtyping cardiac amyloid, augmented by the frequent lack of staining for immunoglobulin light chains. Therefore, the presence of amyloid in the cardiac biopsy should prompt a search for possible plasma cell dyscrasia despite strong transthyretin positivity by immunostaining. Confirmation with MS should be sought if there is any discrepancy between kappa/lambda staining and serum immunofixation results.

324 Immunohistochemical Evaluation of Amyloidosis in Endomyocardial Biopsies.

CD Tan, M Hanna, ER Rodriguez. Cleveland Clinic, OH.

Background: Distinguishing between the different types of amyloid that involves the heart has become increasingly important for therapeutic purposes. While there are at least 27 different proteins that can form amyloid fibrils, the most commonly encountered in cardiac biopsies are immunoglobulin light chains (AL) and transthyretin (ATTR). The limitations of immunohistochemical typing of amyloid in biopsy specimens are well-known. We sought to investigate the utility of immunohistochemical staining in establishing the amyloid type found in endomyocardial biopsies.

Design: Fifty-five cases of amyloidosis were diagnosed on endomyocardial biopsies within a 36-month period. Thioflavin S stain was used to identify amyloid in paraffin-embedded tissue sections. Immunohistochemical staining using a panel of amyloid A, kappa, lambda and transthyretin was performed on all positive biopsies. Sequencing of the transthyretin gene from blood samples was performed in half of the patients with ATTR.

Results: Amyloid typing was possible in 52 of the 55 cases (94%). Two cases were negative for all 4 antibodies; diagnosis was established by electron microscopy in 1 of these cases. Staining results were equivocal in the third case. None of the cases stained with amyloid A. Occasional nonspecific weak staining with light chains was seen in ATTR cases. Conversely, transthyretin does not appear to cross-react with AL amyloidosis.

There is a marked predominance of male patients with amyloidosis of any type (overall M:F ratio is 4:1). Patients with ATTR (mean age 73) are older than AL patients (mean age 66). ATTR was the most common type of amyloid found (n=22), followed by AL of lambda light chains (n=19) and AL of kappa light chains (n=11). Six of 11 ATTR patients were positive for mutations in the transthyretin gene. The most common mutation was Val122Ile. Two of the ATTR patients with organ involvement limited to the heart underwent cardiac transplantation and are alive without disease on 2-year follow-up.

Conclusions: Immunohistochemistry diagnosis of amyloid in endomyocardial biopsies is a reliable method. Molecular genetic testing of transthyretin is a valuable complement to the work-up of these patients.

325 Utility of CD68/CD31 vs. CD163/CD31 Dual Immunostaining Techniques To Detect Antibody-Mediated Rejection in Post-Transplant Cardiac Biopsies.

S Tatishchev, L Czer, J Kobashigawa, D Luthringer. Cedars-Sinai MC, Los Angeles; CSMC, LA.

Background: Antibody-mediated rejection (AMR) in cardiac allograft tissue predicts poor prognosis. There is no gold standard for histologic diagnosis of AMR. Identification of macrophages adherent to the vascular walls on H&E slides is indicative of AMR with ~ 99% specificity and marginal sensitivity (30%). To offset lack of sensitivity, macrophages attached to capillaries have been visualized using antibodies against CD68 & CD31 on paraffin-embedded tissue. This approach has at least 2 intrinsic limitations: 1) Using separate tissue sections for each immunostain precludes the observer's ability to assess identical structures on both slides; 2) CD68 is an organelle-specific (i.e. lysosomes) rather than cell lineage-specific antigen, such as CD163 (macrophage). To simplify visualization of macrophages within capillaries and to assess CD68 vs. CD163 specificity we employed dual staining of paraffinized tissue with CD68/CD31 & CD163/CD31.

Design: 30 cardiac biopsies up to 3 years post-transplant were selected; 6 cases had antibody-mediated rejection (AMR1; as defined by C4d staining) and 24 were negative cases (AMR0). Sections from each case were stained with either a combination of CD68 (red chromogen) & CD31 or a combination of CD163 (red chromogen) & CD31. Dual stains performed on all AMR0 & AMR1 cases were evaluated for ability to unequivocally identify margination of macrophages within capillaries. Dual stains performed on AMR0 cases were evaluated for differences in specificity between CD68 & CD163. To assess specificity, AMR0 cases were blinded, blood vessels highlighted by CD31 on each biopsy section were counted and further stratified based on the presence or absence of distinct red chromogen-positive tissue elements within the vascular walls.

Results: Staining of AMR positive tissue sections with either CD68/CD31 or CD163/CD31 allowed a virtually effortless visualization of macrophages adherent to the capillaries in all cases. Comparison of AMR negative cases showed roughly equal specificities of 97.7% & 96.7% for CD68 & CD163, respectively.

Conclusions: Contrary to our expectations based on the reported antigenic affinities of employed immunostains, both dual staining techniques are equally sensitive and highly specific in detecting intracapillary macrophages. Dual staining using either CD163/CD31 or CD68/CD31 greatly simplifies visualization of macrophages adherent to the capillaries and is helpful for identification of AMR in post-transplant cardiac biopsies.

326 The Pathology of TRI-Tech Leaflet Escape.

M Valente, M Della Barbera, A Angelini, G Cresce, M Montisci, G Thiene. University of Padua, Medical School, Padova, Italy; San Bortolo Hospital, Vicenza, Italy.

Background: The TRI-Tech valve is a low-profile mechanical bileaflet valve prosthesis with a rotating pivot system. Leaflet escape due to pivot fracture was reported and the implantation program interrupted worldwide. The fracture was ascribed to pivot height asymmetry.

Design: To assess whether the asymmetry was an isolated defect or intrinsic to other commercialized TRI-Tech valves, 3 TRI-Tech valves with leaflet dislodgement implanted in 3 patients (pts) two in aortic and one in mitral position and 150 unimplanted TRI-Tech valves, 19-31 mm in size, were studied. Both the pts with aortic escape died suddenly at 10 days and 39 months after surgery and the escaped emidisc was found in the thoracic aorta and in the left common iliac artery, respectively. The pt with mitral leaflet escape had a cardiogenic shock at 22 months, was successfully reoperated and the escaped leaflet was found in the left common iliac artery. Tab height and asymmetry measurement (Δ between tab heights from the leaflet base) was performed in all cases.

Results: In all the escaped discs one pivot disappeared, fractured at the base, thus explaining leaflet dislodgment from the hinge and its distal escape. Small thrombus deposition was observed within the hinge of the fractured tab in the aortic patient who died suddenly at 40 months from reoperation.The asymmetry was over 0.35 mm in all (0.55 and 0.40 mm in the aortic, and 0.46 in the mitral prostheses), and the fracture involved the lower tab in 2 and the higher tab in one. The asymmetry was observed in all unimplanted valves was less than 0.08 mm in 69 (46%), in between 0.08 and 0.20 in 66 (44%), 0.20 to 0.35 mm in 14 cases (9%), and over 0.35 mm in one case. Only in one out of 150 unimplanted valves the asymmetry was as high as observed in the fractured clinical valves.

Conclusions: Asymmetry was present in all unimplanted valves, however, in only one device it was of such size as observed in failing devices. This means that pivot fracture occurred when the height asymmetry was particularly severe. The more the asymmetry the early the fracture occurrence. Pivot rupture with leaflet escape was rarely reported in other valve models. The TRI-Tech quality control did not foresee pivot symmetry check. Since tolerance for pivot asymmetry is unknown and risk of rupture unpredictable, interruption of implant program with prophylactic replacement of implanted TRI-Tech valve was judicious.

327 Chromatin Remodeling and Cell Cycle Activity in Periinfarction Myocardium.

B Ye, W Mao, L McMahon, Q Yang, H Xu, F Li. University of Rochester Medical Center, NY.

Background: Proliferative activity of cardiac myocytes has been observed in periinfarction myocardium. To access DNA template, chromatin remodeling and DNA unwinding is required. Enhancer of zeste homolog 2 (EZH2), a key component of polycomb repressive complex 2, regulates cell proliferation by histone H3 methylation at lysine 27. Brahma-related gene 1 (Brg1) is the ATPase subunit of a large chromatin remodeling complex. The aim of this study was to determine if EZH2 and Brg1 expressed in periinfarction myocardium.

Design: Ten cases of left ventriculectomy for the placement of left ventricle (LV) assistance device in patients with acute myocardial infarction less than 2 week old and 2 cases of normal hearts unsuitable for implantation were studied. Four micron sections of LV were stained with antibodies against EZH2 (Leica, clone 6A10, 1:100), Brg-1 (Santa Cruz, clone G-7, 1:100), and Ki-67 (DAKO, clone MIB1, 1:100) using a kit (EnVison™ Flex+ Dako) and an automated immunostainer.

Results: Rare non-cardiac myocytes in normal hearts and remote areas of infarcted hearts showed nuclear positivity for EZH2 and Ki-67, but no staining for these markers was detected in cardiac myocytes in the same areas. In periinfarction myocardium, there was significant increase in Ki-67 and Brg1 positive non-cardiac myocytes. Strong nuclear staining for these markers was also detected in 5 to 10% cardiac myocytes in periinfarction zones. More importantly, serial section staining revealed that there was co-expression of these markers in cardiac myocytes of periinfarcion myocardium. Brg-1 was weakly expressed in both cardiac myocyte and non-cardiac myocytes in normal hearts and remote areas of infarcted hearts. There was significant increase in Brg-1 expression in periinfarcion myocardium.

Conclusions: Cell cycle entry in cardiac myocytes of periinfarction myocardium is accompanied by increased expression of EZH2 and Brg1. This result suggests there is chromatin remodeling and histone modification in cardiac myocytes of periinfarction myocardium.

327A Novel PKP2 Mutations in Sudden Death Due to Arrhythmogenic Right Ventricular Cardiomyopathy and Sudden Unexpected Death with Normal Cardiac Morphology.

R Zhang, LF Xu, L Li, B Oliveira, AP Burke. University of Maryland, Baltimore.

Background: Sudden deaths in adults are often of cardiac origin and can be attributed to Arrhythmogenic right ventricular cardiomyopathy (ARVC) and sudden adult death syndrome (SADS). ARVC has been linked to mutations in Plakophilin2 (PKP2), which is a desmosome related protein with numerous armadillo repeats. SADS accounts for up to 30% of sudden death in adults, and a subset of cases has also been linked to ion channel mutations, but not to PKP2 thus far. We determined mutational status of PKP2 in a series of patients dying suddenly with ARVC and SADS.

Design: 33 cases of sudden unexpected death of cardiac etiology determined by full forensic autopsy were studied. 7 cases were witnessed sudden deaths in patients with normal hearts; 4 men (aged 32 ± 11) and 3 women (aged 24 ± 16). 26 cases had typical morphologic features of ARVC (fibrofatty infiltrates in the right ventricle and subepicardium of the left ventricle); 19 men (aged 35 ± 17 years) and 7 women (aged 33 ± 16 years). We sequenced all 14 exons of PKP2 in DNA extracted from post-mortem tissues of the 26 patients dying with ARVC and 7 with SADS. The primers used in this study were designed using the Primer Express 3.0 software. Direct sequencing for both sense and antisense strands was performed with a BigDye Terminator DNA sequencing kit on a 3130 Genetic Analyzer with SeqScape software.

Results: PKP2 mutations were identified in 7 of 26 DNA samples from patients with ARVC. Of the 7 mutations, 3 were likely significant, and two of which (L64PfsX22 and N642del) are novel mutations that has not been reported in patients with ARVC. PKP2 mutations were also identified in 3 of 7 cases of SADS, and one novel mutation (F339S) is likely significant.

Conclusions: PKP2 mutations are not specific for ARVC and may also be found in patients with sudden death without morphologic findings (SADS). Three new mutations of PKP2 are described (F339S,N642del,L64PfsX22) in patients with ARVC and SADS.

328 Oxidative Stress and ERK1/2 MAP Kinase Mediate Cardiomyocyte Injury in Transthyretin Cardiac Amyloidosis.

X Zhang, Q Xie, D Tan, PJ Lee, FL Lacbawan, J Libian. State University of New York, Downstate Medical Center, Brooklyn; Yale University School of Medicine, New Haven, CT.

Background: Transthyretin (TTR) is associated with two forms of cardiac amyloidosis: familial (mutant TTR) and systemic senile amyloidosis (wildtype TTR). Approximately 4% of African Americans are heterozygous for V122I variant TTR, a mutation associated with familial amyloidotic cardiomyopathy. The mechanisms of TTR-induced cardiac injury remain elusive. Markers of oxidative stress have been associated with TTR amyloid deposits in peripheral nerve and we previously reported that oxidative stress and ERK1/2 activation mediate cell death in lung epithelium. We investigated the potential role of oxidative stress and ERK1/2 activation in mediating TTR-induced cardiomyocyte injury.

Design: Cases of TTR cardiac amyloidosis and age-matched controls were identified from 2007-2010 autopsy records. TUNEL and 8-OH-dG staining was performed on formalin-fixed paraffin-embedded sections from left ventricle. The TTR gene was sequenced using genomic DNA extracted from the paraffin blocks. Cultured rat cardiomyocytes were exposed to TTR fibrils formed by incubating wildtype TTR under acidic conditions. Apoptosis was assessed by TUNEL staining and Annexin V flow cytometry. Oxidative stress was examined by Western blot for heme oxygenase-1 (HO-1), reactive oxygen species (ROS) production, and 8-OH-dG staining. ERK1/2 activation was measured by Western blot of phospho-ERK1/2.

Results: Four cases of TTR cardiac amyloidosis (average age 82.8 years; range 80 to 87 years) were identified. All patients had presented with chronic heart failure and arrhythmia. TTR gene sequencing identified mutant TTR (V122I) in 3 cases and wildtype TTR in 1 case of cardiac amyloidosis. Positive staining of TUNEL and 8-OH-dG was more prominent in cases of cardiac amyloidosis than in control heart tissue. Rat cardiomyocytes treated with TTR fibrils showed more ROS production, HO-1 expression, phospho-ERK1/2, and apoptosis than untreated cardiomyocytes. Inhibition of ERK1/2 activation by PD98059 or ROS production by diphenylene iodonium ameliorated TTR fibril-induced oxidative injury and apoptosis.

Conclusions: Apoptosis and oxidative injury are increased in hearts of patients with cardiac amyloidosis compared with age-matched controls. Oxidative stress, ERK1/2 activation, and apoptosis are involved in TTR-induced injury of cultured rat cardiomyocytes. Inhibition of oxidative stress and ERK1/2 activation may provide a potential mechanism for prevention and treatment of cardiac injury associated with TTR cardiac amyloidosis.

Cytopathology

329 Heterogeneity of the Testis, an Important Clinical Fact for Infertile Azoospermic Men Undergoing Fine Needle Aspiration of the Testis.

SH Abu-Farsakh, HA Abu-Farsakh. Jordan University, Amman, Jordan; First Medical Lab, Amman, Jordan.

Background: Azoospermic infertile male patients have to resort to testicular fine needle aspiration to search for sperms. These sperms can be used for intracytoplasmic sperm injection into the partner's ova in the assisted reproduction procedure. Finding sperms in the testis is of paramount importance for such couples.

Design: 1620 azoospermic patients had undergone testicular fine needle aspiration for the assessment of their spermatogenesis status. Each patient has been sampled from 10 specific locations, 5 from the right testis and 5 from the left testis, using 27 gauge needles. Patients are classified according to the presence or absences of sperms and its quantity into the following stages: I) Sertoli cells only, II) Spermatogenesis arrest at early stage, III) Spermatogenesis arrest at late stage, IV) sperm heads only V) Hypospermatogenesis (sperms were seen) and VI) Obstructive azoospermia. Hypospermatogenesis is also divided into 4 classes according to the amount of sperms: A) very marked Hypospermatogenesis, B) marked Hypospermatogenesis C) moderate Hypospermatogenesis D) mild Hypospermatogenesis. In each patient, the testis is classified as homogenous or heterogeneous in regard to spermatogenesis status. The testis is considered heterogeneous when 5 testicular sites or less show the cytomorphological changes of the highest stage of spermatogenesis diagnosed in that particular patient.

Results: Patients' ages ranged from 20-55 years with average age 28.5 years. Testicular fine needle aspiration from the 10 sites from each patients showed that the testis was homogenous in 1083 cases (67%) and heterogeneous in 537 cases (33%). The